J Interv Card Electrophysiol (2008) 23:175–181
DOI 10.1007/s10840-008-9300-8

Evaluation of 3D guided electroanatomic mapping for ablation of atrial fibrillation in reference to CT-Scan image integration

Christian de Chillou · Marius Andronache · Ahmed Abdelaal · Yves Ernst · Isabelle Magnin-Poull · Mohamed Magdi · Ning Zhang · Samuel Tissier · Damien Mandry · Cécile Barbary · Denis Régent · Etienne Aliot

Received: 10 April 2008 / Accepted: 4 July 2008 / Published online: 27 September 2008
© Springer Science + Business Media, LLC 2008

Abstract
Background Anatomical guided atrial fibrillation (AF) catheter ablation relies on the assumption that the *left atrium reconstruction anatomy* (LARA) using a 3D mapping system precisely matches the patient's *CT scan anatomy* (*real anatomy*). This study investigates whether this postulation is accurate using CT scan image integration.
Patients and methods Thirty consecutive patients (23 men, mean age=51.9±9.9 years) with symptomatic drug-refractory paroxysmal (n=21) or persistent (n=9) AF underwent a circumferential, 2×2, pulmonary vein (PV) radiofrequency (RF) ablation using the CARTOMERGE system. Left atrium (LA) anatomy was first reconstructed and RF design lines drawn on this LARA. After a CT-scan image of the LA was integrated into the 3D system, RF lesions were deployed 10 ±5 mm outside the PV ostia (PVO) onto the CT-scan LA surface. The match between the actual RF lines and the RF design lines was analyzed off-line after catheter withdrawal.
Results Circumferential RF design lines were divided into four segments encircling both the right and left PVs. Design segments matched the actual RF segments in a proportion varying from 23% up to 83%. A mean of 2.8±1.6 segments per patient were inaccurately designed that extended a mean of 3.8±2.3mm inside the adjacent PV or 6.7±1.8mm inside the left atrial appendage (LAA). Seven patients (23%) had four or more segments incorrectly designed.
Conclusions Our study reveals the inaccuracy of 3D anatomic guided RF ablation with respect to the LA anatomical structures that could be possibly improved when combined with CT-scan image integration.

Keywords Atrial fibrillation · Electroanatomic mapping · Catheter ablation · CT scan image integration

C. de Chillou · M. Andronache · A. Abdelaal · Y. Ernst · I. Magnin-Poull · M. Magdi · N. Zhang · E. Aliot
Department of Cardiology, University Hospital Nancy, Nancy, France

S. Tissier · D. Mandry · C. Barbary · D. Régent
Department of Radiology, University Hospital Nancy, Nancy, France

C. de Chillou (✉)
Département de Cardiologie, Hôpitaux de Brabois, 1, rue du Morvan, 54511 Vandoeuvre lès Nancy, France
e-mail: c.dechillou@chu-nancy.fr

The landmark finding by Haissaguerre et al. [1] that triggers for AF originated in the PVs had the prospect of dramatically simplifying the ablation process. The two validated ablation techniques nowadays are the electrophysiological segmental isolation at the PV ostium (electrophysiological ablation) [2], and the 3D electroanatomic guided circumferential PV ablation (anatomical ablation) [3].

The anatomical ablation technique primarily relies on the assumption that the *LARA* by the 3D mapping system matches the patient's *real anatomy* and is able to correctly define the PVO-LA junction in order to insure complete PV isolation without the undesirable complications. The aim of the present study is to evaluate this anatomical ablation technique and its level of accuracy.

1 Methods

1.1 Patients characteristics

The study population consists of 30 consecutive patients who underwent PV isolation for symptomatic drug-refractory

paroxysmal/persistent (n=21/9) AF of 5.5±4.5 years duration. A mean of 2.9±1.3 antiarrhythmic drugs had failed to control AF prior to the ablation procedure.

There were 23 men and 7 women, with a mean age of 51.9±9.9 years (range, 29–63 years). Two patients had hypertensive cardiomyopathy, two had coronary artery disease, one had hypertrophic cardiomyopathy, one had mild rheumatic mitral stenosis, one had aortic valve prosthesis and 23 had no evidence of structural heart disease. The mean left ventricular EF was 0.62±0.07 (range, 0.45–0.71), and the mean LA size was 43.4± 5.7 mm (range, 29–56 mm).

1.2 Electrocardiographic-gated multislice computed tomography

All patients underwent an ECG-gated (diastolic phase) helical multislice CT scan of the chest one day preceding the electrophysiological study. Images were acquired using an eight-row multidetector CT scanner (GE Light-Speed®, GE Healthcare). A bolus of 140 ml of contrast (Visipaque® 320, Amersham Health, GE Healthcare) was injected in the right cubital vein at a flow rate of 3.5 ml/s, followed by a 60-ml saline chaser bolus. An automated bolus tracking system was used to synchronize the arrival of the contrast material with initiation of the scan. All data were acquired during a single breath-hold of approximately 20 s.

Image reconstruction was performed, where 6 axial images series were reconstructed every 5% of the RR-interval (ranging between time 60% and 85% of the cardiac cycle ≈75%) per patient. Using the standard image reconstruction algorithm, an effective slice thickness of 1.25 mm and a reconstruction increment of 0.6 mm were chosen.

Using specific volume analysis software (cardEP® on the GE Advantages Windows workstation, GE Healthcare), the volumetric data were reconstructed to create 3D models excluding the structures surrounding the heart. Finally, heart segmentation was performed and the 3D structure of interest (LA and PVs) was converted into a 3D shell image and exported to the CARTO™ XP system.

1.3 Electrophysiological study

All patients provided a written informed consent. Oral anticoagulants were replaced on admission by intravenous heparin to maintain a partial-thromboplastin time of 60 to 90 s (control, 30 s), and a transesophageal echocardiogram was performed before each procedure to exclude LA thrombus.

Through a right femoral venous approach, a 5F quadripolar catheter (XTREM®, ELA Medical, Sorin Group) was advanced in the distal coronary sinus; and through an 8F long sheath (PREFACE®, Biosense Webster, Johnson & Johnson), a 4-mm irrigated-tip ablation catheter (NAVISTAR®, Biosense Webster, Johnson & Johnson) was placed transseptally in the LA for detailed mapping and ablation. Subsequently, intravenous heparin was administered at a dose of 0.5 mg/kg, followed by a repeat bolus to ensure an antithrombin coagulation time constantly >240 s. Sedation was obtained with 10 mg nalbuphine intravenous with incremental doses of 5 mg as necessary throughout the procedure. Bipolar electrograms (bandpass, 30 to 500 Hz) were recorded on a multichannel polygraph (LabSystem PRO®, Bard Electrophysiology).

1.4 Study protocol (Fig. 1)

1.4.1 Step 1: 3D mapping

A 3D shell representing the LA was first constructed using an electroanatomic mapping system (CARTO™ XP, Biosense Webster, Johnson & Johnson) during spontaneous rhythm (AF or sinus rhythm) that was the same rhythm by the time of the CT scan image acquisition, with the electrical reference being chosen as a QRS positive peak deflection on the 12-lead ECG. A great attention was paid to acquire the best possible delineation of areas which are critical for the ablation purpose, i.e. LA-PVO junction and the rim of tissue separating the LSPV from LAA. Selective angiography of the PVs was performed using an NIH catheter and hand injection of 10 ml of contrast (Visipaque® 320, Amersham Health, GE Healthcare). To identify the PVs, the mapping catheter was placed deeply into each vein and slowly dragged back to its ostium under fluoroscopic guidance. Along pullback, multiple locations were recorded to tag the veins. The PVO were identified by fluoroscopic visualization of the catheter tip abruptly jumping out of the PVs into the cardiac silhouette with simultaneous appearance of an atrial electrogram in accordance with the selective PVs angiography. Three locations were recorded along the mitral annulus to tag the valve orifice.

1.4.2 Step 2: RF ablation lines design

Encircling the left- and right-sided PVs by continuous RF lesions deployed ≈ 10±5 mm from the PVO was the primary objective of the ablation procedure. The ablation catheter was manipulated on the LARA and new points were selected at sites judged appropriate to deliver RF energy. Those non contiguous sites, tagged as RF design sites, demarcated a left and a right RF oval-shaped design lines around the left and the right PVs respectively.

The operator was blinded to the CT-scan 3D aspect of the LA all along steps 1 and 2.

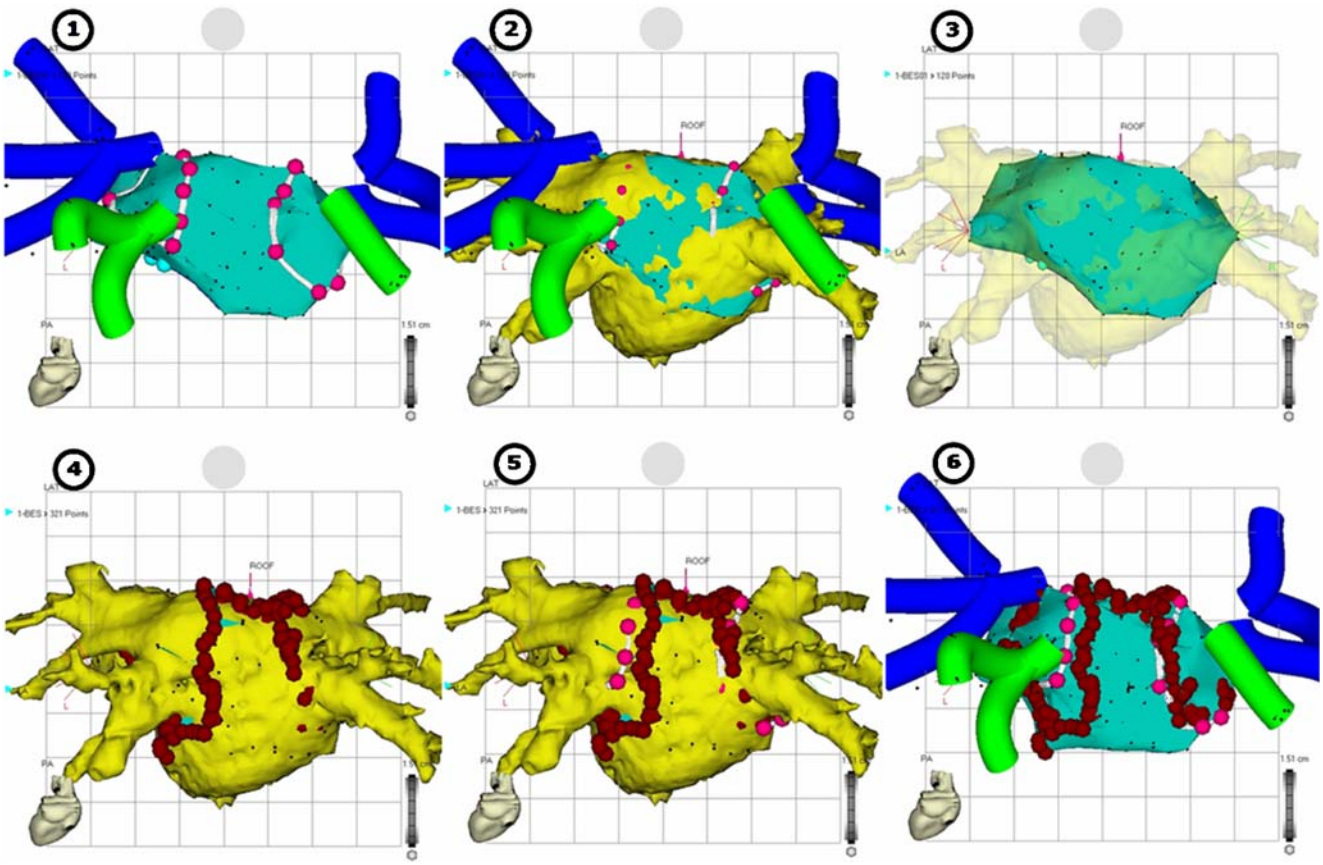

Fig. 1 Illustration of the different phases of the study protocol: *1* electroanatomic mapping is acquired and putative RF lines (*pink tags joined together with white lines*) are designed, *2* left atrial CT-scan is integrated into the LARA 3D map, *3* all 3D mapping tags are masked, *4* the 3D mapping fill threshold is set to zero then RF ablation is performed and each RF application site tagged (*dark brown tags*), *5* all 3D mapping tags are unmasked and *6* left atrial CT-scan image is removed to assess the match between the actual and putative circumferential RF lines

1.4.3 Step 3: CARTOMERGE™ procedure

This process allows the CT image to be placed in the same 3D space in which data is acquired with the CARTO™ XP system. After the LA CT-scan image was incorporated into the real-time map viewer screen of the CARTO™ XP system, a pair of anatomical landmarks (defined as a set of two identical flags attached to both a CT surface image point and a CARTO™ map point) was selected and aligned (visual alignment tool). This anatomical landmark pair was chosen on the LA roof midway between the left and right superior PVO. Finally, the overlap between both the CT scan image and the LARA was obtained by the surface registration process.

1.4.4 Step 4: Radiofrequency ablation

All along the RF ablation procedure, catheter navigation was performed within the CT-scan shell, with the fill threshold of the LARA set to 'zero' and all tagged points masked, in order to locate areas of the LARA that need more point data in order to assure a more accurate reconstruction. Ablation sites were tagged on the LARA model and projected onto the CT scan shell. Circumferential LA lines were created with contiguous coalescent RF lesions delivered at a distance of ≈10±5 mm from the PV ostia. RF current was delivered in unipolar mode by a 550-kHz RF Stockert-Cordis generator via the distal electrode of the irrigated-tip RF catheter. Radiofrequency energy was applied with power limited to 30 W and temperature limited to 48°C using irrigation rates of 18 ml/min (0.9% saline via Cool Flow; Biosense-Webster) until the maximum local electrogram amplitude decreased by >80%.

In addition to the lesions that encircled the left and right-sided PVs, the two circumferential ablation lines were connected with an ablation line along the LA roof and a second line between the LIPV and the mitral valve annulus [4]. The completeness of conduction block across the ablation lines was not routinely assessed.

1.4.5 Step 5: Data analysis

The match between the actual PV circumferential RF lines and the RF design lines delineated in step 2 (see above) was analyzed off-line after catheter withdrawal.

For analysis purpose, each of the design lines was divided into four design segments: anterior/superior, anterior/inferior, posterior/superior and posterior/inferior. A total of eight segments were thus defined (Fig. 2), the anterior and posterior ones demarcating respectively the vicinity of the anterior and posterior aspects of the PVs, the superior and inferior ones demarcating respectively the vicinity of the superior and inferior ipsilateral PVs. The left anterior/superior segment delineates the rim of atrial tissue between the LAA and the LSPV.

The match between each design segment and the corresponding segment on the actual RF lines was analysed using a binary classification: when both were fully superimposed (±5 mm of flexibility) the design segment was classified as accurate, and it was classified as inaccurate when this condition was not fulfilled. Since actual RF lines were deployed 10±5 mm outside from PVO, note that this 5 mm flexibility never permits any design line to be classified as accurate if such a line would cross a PVO.

1.5 Management after ablation

Within 48 h post ablation, all patients were subjected to a control transthoracic echocardiogram, chest CT-scan (to detect early PV stenosis) and 3 days telemetry ECG monitoring. Oral anticoagulation was reinitiated the day after ablation to be maintained for at least 6 months. All patients were discharged on the third day to be followed up on an out-patient basis with regular clinical evaluation and 24-h Holter recordings.

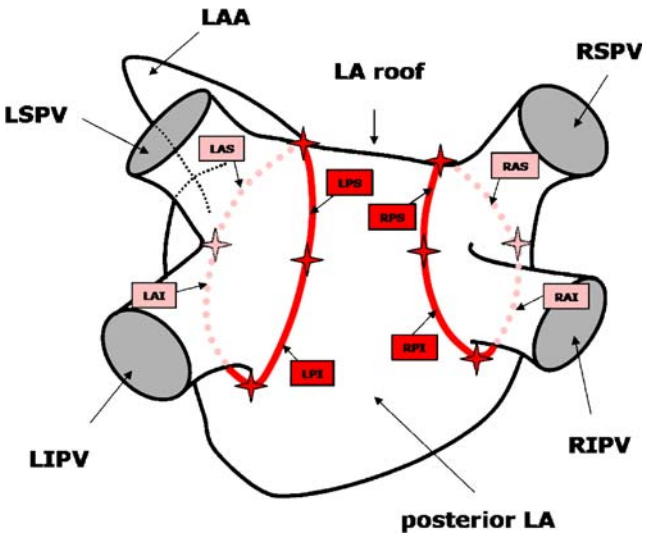

Fig. 2 Schema representing a posterior LA view with the eight segments defining the designed RF lines. *LA* Left atrium, *LAA* left atrial appendage, *LAI* left anterior and inferior, *LAS* left anterior and superior, *LIPV* left inferior pulmonary vein, *LPI* left posterior and inferior, *LPS* left posterior and superior, *LSPV* left superior pulmonary vein, *RAI* right anterior and inferior, *RAS* right anterior and superior, *RIPV* right inferior pulmonary vein, *RPI* right posterior and inferior, *RPS* right posterior and superior, *RSPV* right superior pulmonary vein

2 Results

2.1 Procedural characteristics

Total procedure time was 205±32 min (range: 157 to 273 min) and fluoroscopy time was 18±8 min (range: 5 to 41 min). A mean of 143±40 points (range: 62 to 220 points) were acquired during the LA mapping and RF lines design phases (procedure steps 1 and 2) which together lasted 62± 20 min (range: 20 to 95 min). A mean of 1.2 points per ml of LA volume were acquired for the LARA. The total duration of RF energy application was 51±9 min (range: 40 to 69 min).

The LA volumes were 116±31 ml (range: 64 to 178 ml) as measured on the CT scan images. After step 3 completion, the mean average distance between the LARA and the CT scan anatomy shells was 2.14±1.53 mm (range: 1.75 to 3.52 mm).

There were no procedural complications except for one case of mild pericardial effusion (<8 mm) managed medically.

2.2 Validation of RF design lines

Depending on their location, design segments matched the actual RF line segments in a proportion varying from 23% up to 83% (Table 1).

The worst match was observed for the left anterior/superior segment with only seven out of 30 segments (23%) accurately drawn. This segment corresponds to the rim of atrial tissue separating the LSPV from the LAA. Among the remaining 23 inaccurately drawn segments, ten extended within the LAA (Fig. 3), ten within the LSPV and three were drawn within a portion of both the LAA and the LSPV. The inaccurate segments extended a mean of 5.7± 2.4 mm beyond the LSPV ostium and a mean of 6.7± 1.8 mm beyond the LAA entrance. The second worst matching segment was the left posterior/superior one, with 17 out of 30 segments (57%) accurately drawn.

For all non matching segments, inaccuracy corresponded to an extension within the adjacent PV or LAA, but never outside the 10mm width imaginary strips surrounding the PV on which the RF lesions were actually deployed. Segments could extend as deep as 12 mm within a given PV (3.8±2.3 mm on average).

When analyzing the results on PV basis, the percentages of PV accurately encircled were 17% (5/30), 60% (18/30), 60% (18/30) and 50% (15/30) for the LSPV, LIPV, RSPV and RIPV respectively.

Table 1 Comparison between design and actual RF ablation lines

Segments	Inaccurate segments	Mean distance outside PVO (mm)	Mean distance inside PVO (mm)	Mean distance inside LAA (mm)
Left PVs				
Anterior/superior	23/30 (77%)	NM[a]	5.7±2.4 (n=13[a]), range, 2–10	6.7±1.8 (n=13[a]), range, 4–10
Anterior/inferior	9/30 (30%)	4.8±2.2, range, 2–10	4.7±2.2, range, 1–9	4.7±1.8 (n=7), range, 2–8
Posterior/inferior	8/30 (27%)	4.0±1.5, range, 2–7	2.3±1.5, range, 1–5	NA
Posterior/superior	13/30 (43%)	3.5±2.3, range, 1–8	3.8±3.1, range, 2–12	NA
Right PVs				
Anterior/superior	10/30 (33%)	4.4±3.2, range, 1–14	3.5±1.8, range, 1–7	NA
Anterior/inferior	8/30 (27%)	6.2±3.5, range, 2–15	3.3±1.0, range, 2–5	NA
Posterior/inferior	5/30 (17%)	4.3±2.3, range, 1–10	3.4±1.8, range, 1–6	NA
Posterior/superior	5/30 (17%)	4.6±2.9, range, 1–11	2.6±1.5, range, 1–5	NA

LAA Left atrial appendage, *NA* not applicable, *NM* not measurable, *PVO* pulmonary vein ostium

[a] See explanations in the text

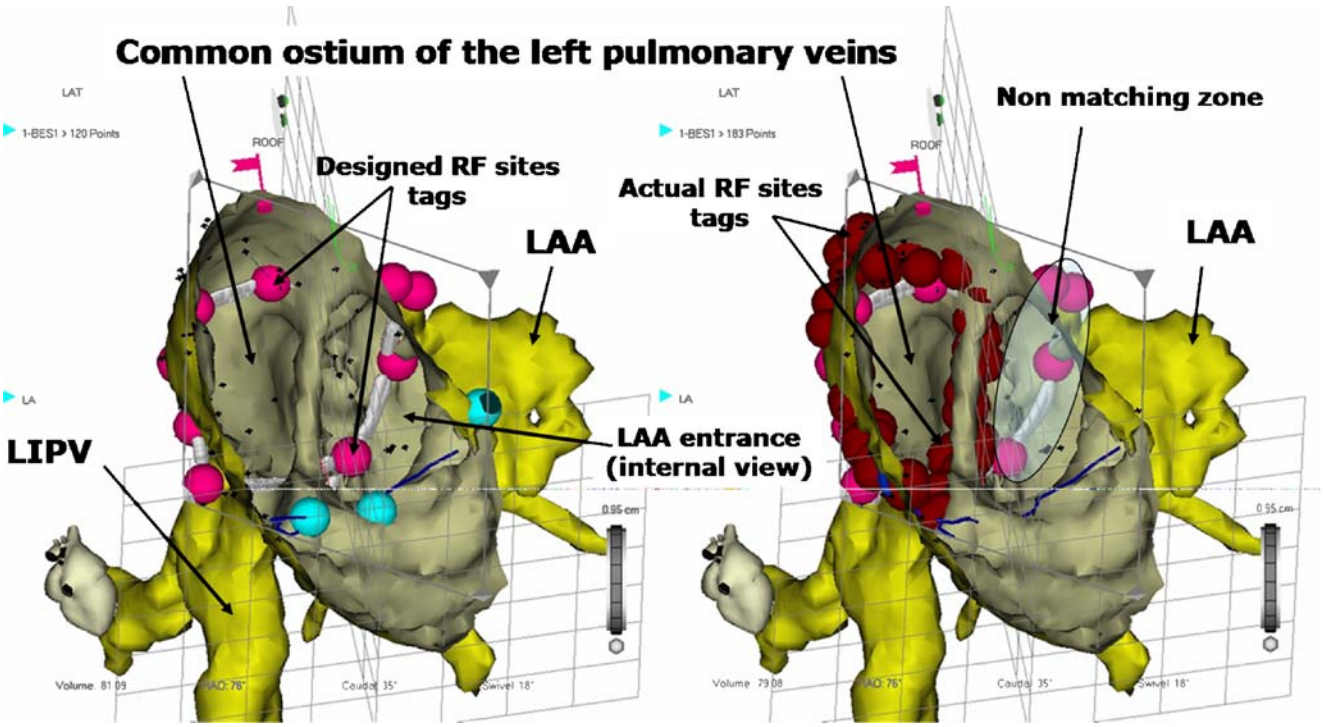

Fig. 3 Example of a 3D CT-scan clipping plane (right lateral oblique view) of the LA in a particular patient in whom the designed and the actual RF lines around the left pulmonary veins did not match. The *pink tags joined together with white lines* (*left and right pictures*) represent the designed RF line encircling the left veins whereas the *joined dark brown tags* represent the actual RF line (*right picture*). Based upon the LARA map, RF energy would have been wrongly delivered 10 mm deep in the LAA

When analyzing the results on a patient basis, a mean of 2.8±1.6 segments per patient (ranging from 0 to 7) were inaccurately designed. Only one patient had all segments perfectly matching the subsequent RF line segments, but seven patients (23%) had four or more segments inaccurately designed.

2.3 Clinical Outcome

At a mean follow-up of 4.6±1.6 months (range 3 to 7), 20 patients (16 without antiarrhythmic drugs) were free of arrhythmia-related symptoms and had no atrial arrhythmia recurrence documented on Holter monitoring. The remaining ten patients were documented with AF recurrence (n=9), atypical atrial flutter (n=1) or both (n=2).

3 Discussion

This study investigates the accuracy of circumferential RF ablation of PVs using the 3D anatomic guided LARA in reference to the CT-scan image integration.

We found that the RF lines that have been deployed on the 3D guided LARA deviated from the anatomical PVO in 56 out of the 120 target PVs; which might result in harmful and potential risks such as PV stenosis and/or LAA perforation. Our study suggests that integration of CT scan anatomy 3D images is of great help in guiding the anatomical AF ablation technique using the CARTO™ mapping system.

Our findings correlates with the recent study of Perez-Castellano et al. [5] who demonstrated a significant deviation between the PVO definition based upon the 'standard' CARTO™ system (i.e.: without the CARTOMERGE™ technology) as compared to the CT scan anatomy unmasked by PV angiograms. Perez-Castellano et al. [5] found that 80% of PV ostia location estimations were wrongly tagged inside the PV.

The difficulty of a circumferential ablation around the anterior aspect of the left PVs is due to the narrow ridge that separates the LSPV from the adjacent appendage, a remark which had been already raised and demonstrated by many authors [6] using gadolinium-enhanced cardiac magnetic resonance imaging. Our study confirms this finding with the lowest percentage (23%) of putative RF lesions correctly deployed on that same segment.

Tops et al. [7] demonstrated the feasibility of fusion of CT-scan images with 3D electroanatomic mapping in patients undergoing catheter ablation for AF and found a mean 2.0±0.2 mm distance only between the CT scan anatomy and the LARA map. Dong et al. [8] reported a position error of 2.1±1.2 mm for PV ablation using an electroanatomical approach with CT-scan integration in an animal model. Our data showing a mean 2.14±1.53 mm distance between CT scan and electroanatomical shells is pretty similar to these early publications. Although all the above studies; including our study have almost the same mean matching statistical value between the CT scan image and the LARA image, a real time 3D imaging modalities may be further required to assess the accuracy of the CT scan image integration technique.

3.1 Study limitations

First, the LARA maps and the CT scan images were not done at the same moment in time which may result in errors that can be overruled during the registration technique. In a trial to minimize this error in our study, both procedures were carried less than 24 h apart.

It has been determined that craniocaudal cardiac motion is the main movement seen during respiration [9]. Noseworthy et al. quantitative assessment of 3D images during respiratory phases revealed splaying of the PVs and reduction in their caliber mainly during held inspirations [9]. For this reason, CT-scan acquisition and selective PV angiography done for defining the PVO on the LARA were all carried in our study during held expiration in order to minimize this error as possible.

The effect of the difference of cardiac rhythm at the time of the CT-scan image acquisition and the mapping procedure on the LA anatomy has been minimized in our study. Only patients with the same cardiac rhythm during the mapping procedure and the CT-scan acquisition time were included in our study. Additionally, it had been proved that the cardiac rhythm had no significant effect on the total or regional registration accuracy [10].

The other factor that may affect the LA size is the hydration status of the patient especially in patients with pulmonary congestion (as those with congestive heart failure and mitral regurge) after long periods of supine position [11]. To minimize this effect, patients with mitral regurge and congestive heart failure were not included in our study.

The above factors may have contributed to minimize a possible biologic-related distortion between the CT and electroanatomical shells in our study: CT-scan acquisitions were ECG-gated and electroanatomic mapping were performed using also a QRS complex as the electrical reference.

4 Conclusions

Our work demonstrates the inaccuracy of the 3D anatomic guided LARA maps for delineation of the PVO-LA tissue landmarks with its potential impact on the outcome of the ablation procedure. CT-scan image integration may represent an additive tool to increase the accuracy of this technique.

References

1. Haïssaguerre, M., Jaïs, P., Shah, D. C., Takahashi, A., Hocini, M., Quiniou, G., et al. (1998). Spontaneous initiation of atrial fibrillation by ectopic beats originating in the pulmonary veins. *The New England Journal of Medicine*, *339*, 659–666.
2. Haïssaguerre, M., Shah, D. C., Jaïs, P., Hocini, M., Yamane, T., Deisenhofer, I., et al. (2000). Electrophysiological breakthroughs from the left atrium to the pulmonary veins. *Circulation*, *102*, 2463–2465.
3. Pappone, C., Rosanio, S., Oreto, G., Tocchi, M., Gugliotta, F., Vicedomini, G., et al. (2000). Circumferential radiofrequency ablation of pulmonary vein ostia: A new anatomic approach for curing atrial fibrillation. *Circulation*, *102*, 2619–2628.
4. Jaïs, P., Hocini, M., Hsu, L. F., Sanders, P., Scavée, C., Weerasooriya, R., et al. (2004). Technique and results of linear ablation at the mitral isthmus. *Circulation*, *110*, 2996–3002.
5. Perez-Castellano, N., Villacastin, J., Moreno, J., Rodriguez, A., Moreno, M., Conde, A., et al. (2005). Errors in pulmonary vein identification and location in the absence of pulmonary vein imaging. *Heart Rhythm*, *2*, 1082–1089.
6. Kato, R., Lickfett, L., Meininger, G., Dickfeld, T., Wu, R., Juang, G., et al. (2003). Pulmonary vein anatomy in patients undergoing catheter ablation of atrial fibrillation: Lessons learned by use of magnetic resonance imaging. *Circulation*, *107*, 2004–2010.
7. Tops, L. F., Bax, J. J., Zeppenfeld, K., Jongbloed, M. R. M., Lamb, H. J., ven der Wall, E. E., et al. (2005). Fusion of multislice computed tomography imaging with three-dimensional electroanatomic mapping to guide radiofrequency catheter ablation procedures. *Heart Rhythm*, *2*, 1076–1081.
8. Dong, J., Calkins, H., Solomon, S. B., Lai, S., Dalal, D., Lardo, A., et al. (2006). Integrated electroanatomic mapping with three-dimensional computed tomographic images for real-time guided ablations. *Circulation*, *113*, 186–194.
9. Noseworthy, P. A., Malchano, Z. J., Ahmed, J., Holmvang, G., Ruskin, J. N., & Reddy, V. Y. (2005). The impact of respiration on left atrial and pulmonary venous anatomy: Implications for image-guided intervention. *Heart Rhythm*, *2*, 1173–1181.
10. Kistler, P. M., Earley, M. J., Harris, S., Abrams, D., Ellis, S., Sporton, S. C., et al. (2006). Validation of three-dimensional cardiac image integration: Use of integrated CT image into electroanatomic mapping system to perform catheter ablation of atrial fibrillation. *Journal of Cardiovascular Electrophysiology*, *17*, 341–348.
11. Pape, L. A., Price, J. M., Alpert, J. S., Ockene, J. S., & Weiner, B. H. (1991). Relation of left atrial size to pulmonary capillary wedge pressure in severe mitral regurgitation. *Cardiology*, *78*, 297–303.